



X=Y=ZH Systems as potential 1,3-dipoles. Part 58: Cycloaddition route to chiral conformationally constrained (*R*)-pro-(*S*)-pro peptidomimetics

H. Ali Dondas,^{a,b} Ronald Grigg^{a,*} and Colin Kilner^a

^aDepartment of Chemistry, Molecular Innovation, Diversity and Automated Synthesis (MIDAS) Centre, School of Chemistry, The University of Leeds, Leeds LS2 9JT, UK

^bDepartment of Chemistry, Faculty of Pharmacy, Mersin University, 33342 Mersin, Turkey

Received 14 July 2003; revised 22 August 2003; accepted 11 September 2003

Abstract—Imines of (1*S*,9*S*)-*t*-butyl-9-amino-octahydro-6,10-dioxo-6*H*-pyridazino[1,2-*a*][1,2]diazepine-1-carboxylate undergo thermal (toluene, 110°C) or LiBr-DBU catalysed (MeCN, room temperature) regio- and stereo-specific cycloaddition to a range of chiral dipolarophiles giving enantiopure spiro-cycloadducts in excellent yield. The reactions proceed via intermediate NH azomethine ylides and litho azomethine ylides, respectively and results in the multiplication of chiral centres from 2 (one of which is lost in the process) to 5. © 2003 Elsevier Ltd. All rights reserved.

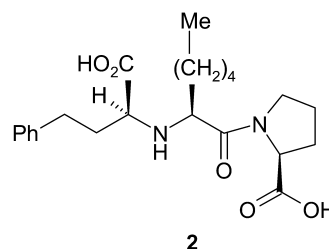
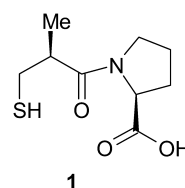
The strong and continuing interest in peptidomimetics has been given a substantial boost by the emerging importance of the proteome.¹ Special interest attaches to conformationally constrained building blocks that mimic the β -turn motif.²

Drug discovery programs aimed at inhibitors of the zinc metalloprotease, angiotensin-converting enzyme (ACE), resulted in a range of drugs such as captopril **1**, lisinopril **2** and cilazapril **3** that are effective in the treatment of essential hypertension and other cardiovascular and renal disorders.^{3,4} Recently, a novel human zinc metalloprotease, ACE2, has been reported⁵ which in an essential regulator of heart function.⁶ There is significant structural homology between ACE and ACE2,⁷ and this has encouraged us to explore peptidomimetics based on cilazapril.⁸

A substantial amount of novel chemistry, mainly targeted at ACE inhibitors, has been developed from the parent 9-aminopyridazino diazepine carboxylic acid **4a**, the corresponding *t*-butyl ester **4b** and related bicyclic compounds.^{8–10}

Our thermal and metal catalysed^{11–13} imine-azomethine ylide-cycloaddition cascade chemistry has provided a series of cephalosporin analogues¹⁴ and spirobenzodiazepines related to MK-329¹³ and potentially offers a facile route

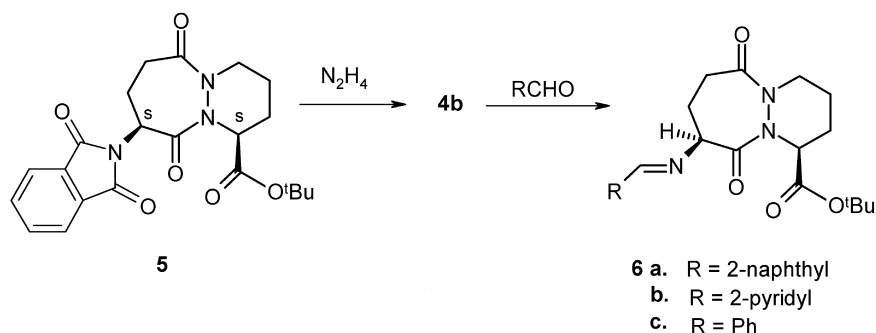
conformationally restricted pro-pro peptidomimetics. To explore this possibility we selected the ala-pro mimetic **4b**, a key intermediate in the synthesis of cilazapril **3**. Elegant ¹H NMR studies on **4a** and **4b** have shown the CO₂H and CO₂Bu^{*t*} groups to be axial and the pyridazine to have a locked chair conformation.¹⁰ Furthermore the conformation of the diazepine ring is locked due to the two amide bonds in conjunction with the chair locked pyridazine.



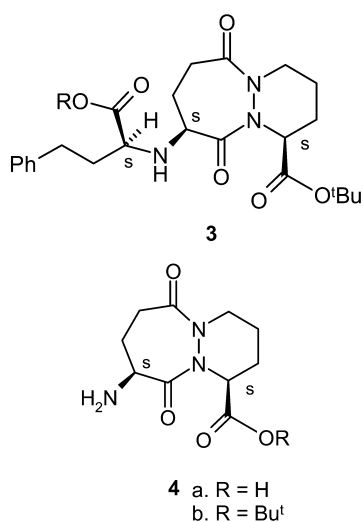
Thus a series of imines **6a–c** (Scheme 1) was prepared from **4b** which was liberated from its phthalimido *t*-butyl ester **5**¹⁵ by treatment with hydrazine hydrate. The imines were then evaluated in thermal and metal catalysed cycloaddition reactions with respect to regio-, diastereo- and enantioselectivity.

Keywords: cilazapril; ACE inhibitors; imines; azomethine ylide; 1,3-dipolar cycloaddition; peptidomimetics; multiplication of chirality.

* Corresponding author. Tel.: +44-1133436501; fax: +44-1133436530; e-mail: r.grigg@chemistry.leeds.ac.uk

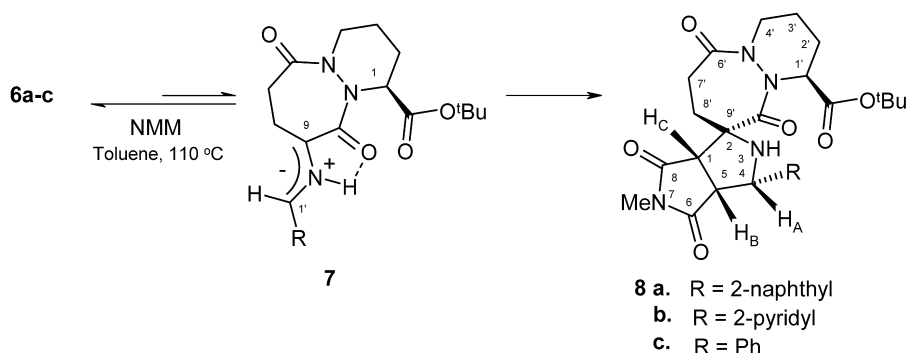


Scheme 1.



1. Thermal cycloaddition

The imines **6a–c** of *t*-butyl 1*S*,9*S*-9-amino-octahydro-6,10-dioxo-6*H*-pyridazino[1,2-*a*][1,2]diazepine-1-carboxylate underwent thermal (toluene, 110°C) regio- and diastereospecific cycloaddition to *N*-methylmaleimide (NMM) to give enantiopure spiro-cycloadducts **8a–c** in 84–93% yield with concomitant increase in the number of chiral centres from 2 to 5 (Scheme 2). The reaction proceeds via a formal 1,2-prototropy generating intermediate NH azomethine ylide **7** in which the original C(9) chirality is destroyed. Hence, the enantioselectivity of these cycloaddition is controlled solely by the C(1) centre and the locked conformation of the bicyclic system.



Scheme 2.

During these cycloadditions a pale green colour develops and is then largely discharged suggesting it is associated with the resonance stabilised azomethine ylide **7** which arises via formal 1,2-prototropy of the C(9)–H. The *cis*-stereochemistry of H_A, H_B and H_C was readily established from n.O.e data (see Section 4) and conforms to that expected^{13,16–18} whilst the C(2)-stereochemistry is assigned on the basis of previous studies^{14,16–18} and an X-ray crystal structure of **8a** (Fig. 1).

The formation of single stereoisomers in these kinetically controlled cycloadditions indicates steric shielding of one face of the azomethine ylide **7** (Scheme 2) by the puckered dioxo-diazepine ring. This shielding effect is also apparent in the crystal structure of **8a** (Fig. 1) in which the dihedral angle between the planes of two amide moieties N(1)–C(7)–O(7) and N(2)–C(11)–O(11) is 63.2°. This compares with a predicted angle from ¹H NMR and modelling of 60°. A further feature of the cycloaddition is that the new C–C bond formed at C(9) replaces the C(9)–H with ‘retention’ of configuration but the chiral descriptor for this site changes to R due to stereochemical preference rules. Thus **8a–c** arise from *endo*-cycloaddition to the 9-*Re*, 1′-*Si* face of the anti-dipole **7** and in **8a–c** the new stereocentres are 1*S*, 2*R*, 4*S*, and 5*R*.

2. Metal ion catalysed cycloaddition

The imines **6a–c** undergo LiBr-DBU catalysed (MeCN, room temperature) regio- and stereo-specific cycloaddition to a range of achiral and chiral dipolarophiles giving enantiopure spiro-cycloadducts in excellent yield via litho azomethine ylides. Thus imines **6a** and **6c** react regio- and

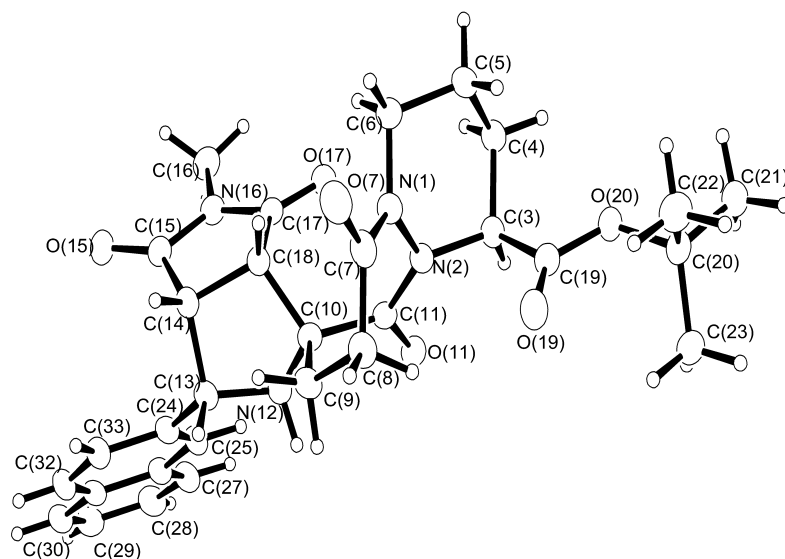
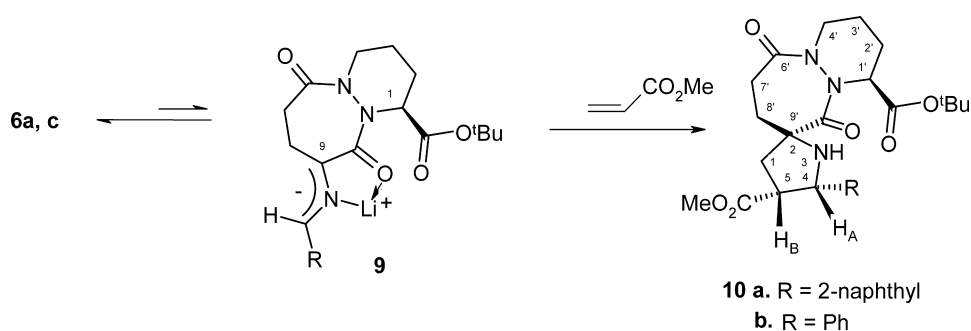


Figure 1. X-Ray crystal structure of **8a**.



Scheme 3.

stereo-specifically with methyl acrylate under the influence of lithium bromide and DBU in acetonitrile over 3.5 h to give single cycloadducts **10a** and **10b** in 82 and 86% yield, respectively (Scheme 3).

In these reactions a green colour develops immediately the imine is contacted with LiBr-DBU and this colour discharges as the reaction proceeds. This colour is believed to arise from the lithio dipole **9**. The stereochemistry of **10a** and **10b** was assigned on the basis of 2-D Cosy studies and an X-ray crystal structure of an analogue (*vide infra*). In these cases an analogous facial shielding effect to that discussed previously is operating and since the stereochemistry of the metallo azomethine ylide **9** is analogous to that of **7**, the stereochemical outcome of Scheme 3 is identical to that of Scheme 2. The new stereocentres are thus *2R*, *4S*, *5R*.

A second series of cycloadducts was prepared from imines **6a–c** and the chiral dipolarophile (*R*)-5(*1R*)-menthyloxy-2-(*5H*)-furanone **11** (Scheme 3). Reaction of **6a–c** with **11** occurred over 3–6 h at room temperature in acetonitrile using lithium bromide-DBU as the catalyst. Enantiopure cycloadducts **12a–c** were obtained as single stereoisomers in 81–93% yield. The stereochemistry of **12a–c** is based on a single crystal X-ray structure of **12c** (Fig. 2) and 2-D Cosy studies. In these reactions the stereochemistry of the cycloaddition is as observed in the previous two series discussed above. Once again the process proceeds via an

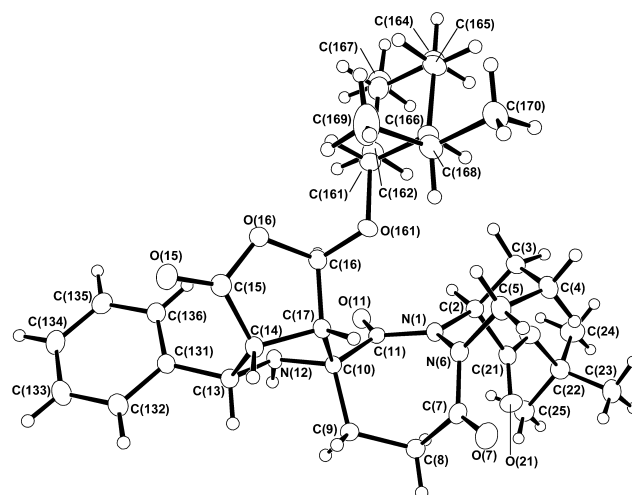
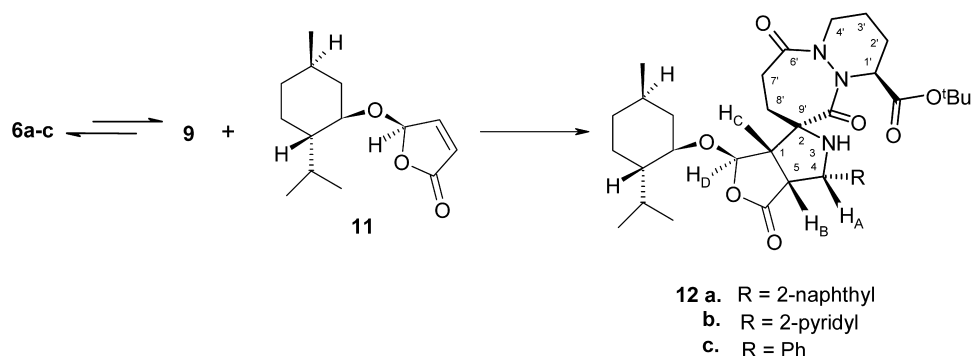


Figure 2. X-Ray crystal structure of **12c**.

endo transition state and as expected the lithio azomethine ylide adds to the face of the dipolarophile **11** *trans* to the *O*-menthyl group.¹⁸ Hence, the newly created stereocentres are *1S*, *2R*, *4S*, and *5R* (Scheme 4).

3. Conclusions

Imines derived from amine **4b** undergo stereo- and



Scheme 4.

regio-specific thermal and metallo-azomethine ylide cascade cycloaddition reactions giving enantiopure products which are (*R*)-pro-(*S*)-pro peptidomimetics bearing two or three additional chiral centres in the newly created proline moiety. A flexible approach to a wide range of potentially bioactive peptidomimetics has been developed.

4. Experimental

Melting points were determined on a Kofler hot stage apparatus and are uncorrected. Mass spectra were recorded at 70 eV on a VG Autospec mass spectrometer. Nuclear magnetic resonance spectra and decoupling experiments were determined at 300 and 400 MHz on a Bruker spectrometers as specified. Chemical shifts are given in parts per million (δ) downfield from tetramethylsilane as internal standard. Spectra were determined in deuteriochloroform except where otherwise stated. The following abbreviations are used; s=singlet, d=doublet, t=triplet, q=quartet, m=multiplet, br=broad and brs=broad singlet. Flash column chromatography was performed using silica gel 60 (230–400 mesh). Kieselgel columns were packed with silica gel GF₂₅₄ (Merck 7730). Petroleum ether refers the fraction with bp 40–60°C unless otherwise specified. Microanalyses were obtained using a Carlo-Erba Model 1106 instrument. Optical rotations were determined on an Optical Activity Ltd., AA1000 polarimeter. (*R*)-5-(1*R*)-Menthylxy-2-(5*H*)-furanone was purchased from Aldrich and used as received.

4.1. General procedure for imine formation

A mixture of aldehyde (1 equiv.), amine (1.05 equiv.) and activated 4 Å molecular sieves in dry DCM was stirred either at room temperature or 40°C for an appropriate time (6–7 h). After removal of the molecular sieves the solvent was evaporated under reduced pressure (bath temperature not higher than 30°C) and the residue crystallised from an appropriate solvent.

4.1.1. (1*S*,9*S*)-9-[(Naphthalen-2-ylmethylene)-amino]-6,10-dioxo-octahydro-pyridazino[1,2-*a*][1,2]diazepine-1-carboxylic acid *tert*-butyl ester **6a.** The product (93%) crystallised from ether–petroleum ether as colourless prisms, mp 151–153°C. $[\alpha]_D^{20} = -71$ (0.5 g/100 mL, EtOH). Found: C, 67.4; H, 6.9; N, 9.15, C₂₅H₂₉N₃O₄·0.5H₂O requires:

C, 67.55; H, 6.75; N, 9.45%; δ (300 MHz): 8.41 (s, 1H, CH=N), 8.1–7.42 (m, 7H, ArH), 5.39 (m, 1H, 1 α), 4.65 (m, 1H, 9 α), 4.35 (m, 1H, 4 β), 3.61 (m, 1H, 7 β), 2.81 (m, 1H, 4 α), 2.65–2.15 (m, 4H, 2 β , 7 α , 8 α , 2 β), 1.95–1.53 (m, 3H, 2 α , 3 α , 3 β), 1.40 (s, 9H, O^tBu); *m/z* (%): 435 (M⁺, 12), 379 (23), 223 (100), 194 (64), 114 (26), 85 (72), 57 (88) and 41 (78).

4.1.2. (1*S*,9*S*)-6,10-Dioxo-9-[(pyridin-2-ylmethylene)-amino]-octahydro pyridazino [1,2-*a*][1,2]diazepine-1-carboxylic acid *tert*-butyl ester **6b.** The product (89%) precipitated from ether–petroleum ether as a pale yellow amorphous solid, mp 87–89°C; $[\alpha]_D^{20} = -109.2$ (1 g/100 mL, EtOH). HRMS (EI), found: 386.1949, C₂₀H₂₆N₄O₄ requires: 386.1954; δ (300 MHz): 8.61 and 8.15 (2 \times d, 2 \times 1H, pyridine-H), 8.32 (s, 1H, CH=N), 7.72 and 7.31 (2 \times m, 2H, pyridine-H), 5.41 (m, 1H, 1 α), 4.70 (m, 1H, 9 α), 4.40 (m, 1H, 4 β), 3.65 (m, 1H, 7 β), 2.81 (m, 1H, 4 α), 2.67–2.20 (m, 4H, 2 β , 7 α , 8 α , 2 β), 2.02–1.60 (m, 3H, 2 α , 3 α , 3 β), 1.42 (s, 9H, O^tBu); *m/z* (%) (FAB): 387 (M+1, 100), 331 (35), 202 (32) and 131 (21).

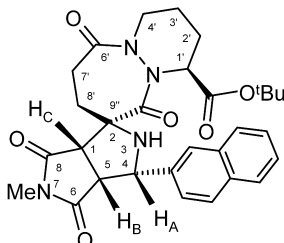
4.1.3. (1*S*,9*S*)-9-(Benzylidene-amino)-6,10-dioxo-octahydro-pyridazino[1,2-*a*][1,2]diazepine-1-carboxylic acid *tert*-butyl ester **6c.** The product (91%) was obtained as pale yellow thick oil, $[\alpha]_D^{20} = -178.6$ (0.3 g/100 mL, EtOH). HRMS (EI), found: 385.2000, C₂₁H₂₇N₃O₄ requires: 385.2000; δ (300 MHz): 8.28 (s, 1H, CH=N), 7.93–7.32 (m, 5H, ArH), 5.38 (m, 1H, 1 α), 4.62 (m, 1H, 9 α), 4.31 (m, 1H, 4 β), 3.60 (m, 1H, 7 β), 2.79 (m, 1H, 4 α), 2.61–2.13 (m, 4H, 2 β , 7 α , 8 α , 2 β), 1.90–1.50 (m, 3H, 2 α , 3 α , 3 β), 1.39 (s, 9H, O^tBu); *m/z* (%) (FAB): 386 (M+1, 100), 330 (51), 197 (17), 130 (51), 91 (12) and 55 (9).

4.2. General procedure for thermal cycloaddition

A solution of imine (1 mmol), and *N*-methylmaleimide (1 mmol) in dry degassed toluene (30 mL) was boiled under reflux under a nitrogen atmosphere for 9–16 h. The solvent was then evaporated under reduced pressure and the residue crystallised from an appropriate solvent.

4.2.1. Cycloadduct **8a (1*S*,2*R*,4*S*,5*R*,1'*S*).** After a reaction time of 14 h and work up the product (89%) crystallised from dichloromethane–hexane as colourless prisms, mp 135–137°C. $[\alpha]_D^{20} = -198.4$ (0.5 g/100 mL, EtOH). Found: C, 64.45; H, 6.15; N, 9.75, C₃₀H₃₄N₄O₆·0.5H₂O requires: C, 64.85; H, 6.30; N, 10.1%; δ (400 MHz): 7.75–7.40 (m, 5H, Ar-H), 5.5 (m, 1H, H1'), 4.71 (dd, 1H, *J*=3.9, 9.4 Hz, H_A), 4.49 (m, 1H, H4'), 3.81 (m, 1H, H7'), 3.50 (dd, 1H, *J*=7.1,

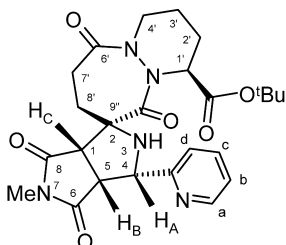
9.4 Hz, H_B), 3.24 (d, 1H, *J*=7.1 Hz, H_C), 3.15 (m, 1H, H₄''), 2.66 (s, 3H, NMe), 2.4 (br, 1H, NH), 2.35 (m, 1H, H₈''), 2.2–1.95 (m, 4H, H₂', H₂'', H₈', H₇''), 1.71 (m, 1H, H₃'), 1.65 (m, 1H, H₃'') and 1.46 (s, 9H, O^tBu); *m/z* (%) (FAB): 547 (M+1, 93), 491 (76), 333 (58), 242 (41), 85 (48) and 57 (100).



n.O.e data:

Signal	Enhancement(%)				
	H _A	H _B	H _C	Ar-H	NH
Irradiated					
H _A		10.3		5.5	2.8
H _B	10.6		8.8		
H _C		14.2			

4.2.2. Cycloadduct 8b (1S,2R,4S,5R,1'S). Work up after a reaction time of 14 h afforded the product (84%) which crystallised from ether–ethanol as colourless prisms, mp 215–217°C. $[\alpha]_D^{20} = -188.8$ (0.5 g/100 mL, EtOH). Found: C, 60.5; H, 6.4; N, 13.9, C₂₅H₃₁N₅O₆ requires: C, 60.35; H, 6.30; N, 14.05%. δ (400 MHz): 8.45 (d, 1H, pyridine-H_a), 7.7 (t, 1H, pyridine-H_c), 7.35 (d, 1H, pyridine-H_d), 7.5 (m, 1H, pyridine-H_b), 5.5 (t, 1H, *J*=5.4 Hz, H₁'), 4.72 (d, 1H, *J*=9.4 Hz, H_A), 4.50 (m, 1H, H₄''), 3.9 (m, 1H, H₇''), 3.69 (dd, 1H, *J*=6.9, 9.4 Hz, H_B), 3.44 (d, 1H, *J*=7.1 Hz, H_C), 3.25 (m, 1H, H₄'), 3.0 (br, 1H, NH), 2.76 (s, 3H, NMe), 2.5 (m, 1H, H₈''), 2.4–2.15 (m, 4H, H₂', H₂'', H₈', H₇''), 1.8 (m, 1H, H₃'), 1.6 (m, 1H, H₃'') and 1.47 (s, 9H, O^tBu) *m/z* (%) (FAB): 498 (M+1, 54), 442 (27), 368 (16), 284 (31), 68 (67) and 55 (100).



n.O.e data:

Signal	Enhancement(%)			
	H _A	H _B	H _C	Ar-H
Irradiated				
H _A		13.0		13.1
H _B	11.5		11.6	
H _C		18.8		

4.2.3. Cycloadduct 8c (1S,2R,4S,5R,1'S). After a reaction time of 16 h and work up the product (93%) precipitated

from ether–petroleum ether as a colourless prisms, mp 105–107°C. $[\alpha]_D^{20} = -103.2$ (0.5 g/100 mL, EtOH). HRMS (EI), found: 496.2318, C₂₆H₃₂N₄O₆ requires: 496.2322; δ (300 MHz): 7.30 (m, 5H, Ar-H), 5.52 (t, 1H, *J*=5.3 Hz, H₁'), 4.65 (dd, 1H, *J*=9.3, 3.0 Hz, H_A), 4.45 (m, 1H, H₄''), 3.91 (m, 1H, H₇'), 3.58 (dd, 1H, *J*=7.0, 9.3 Hz, H_B), 3.33 (d, 1H, *J*=7.0 Hz, H_C), 3.22 (m, 1H, H₄'), 2.95 (br, 1H, NH), 2.78 (s, 3H, NMe), 2.68 (m, 1H, H₈''), 2.41–2.16 (m, 4H, H₂', H₂'', H₈', H₇''), 1.82 (m, 1H, H₃'), 1.6 (m, 1H, H₃'') and 1.49 (s, 9H, O^tBu); *m/z* (%) (FAB): 497 (M+1, 15), 441 (18), 367 (5), 283 (19), 81 (59), 69 (75) and 55 (100).

4.3. General procedure for the lithium bromide catalysed cycloaddition reactions

A mixture of the imine (1 mmol), DBU (1.1 mmol), dipolarophile (1 mmol) and LiBr (1.5 mmol) in freshly distilled acetonitrile (30 mL) was stirred at room temperature under an atmosphere of nitrogen until reaction was complete. The reaction mixture was then quenched by addition of saturated aqueous ammonium chloride solution, and extracted with methylene chloride (2×). The combined organic layers were washed with brine, dried (MgSO₄), filtered and the solvent evaporated. The residue was crystallised from an appropriate solvent.

4.3.1. Cycloadduct 10a (2R,4S,5R,1'S). After a reaction time of 3.5 h and work up the product (82%) precipitated from petroleum ether (60–80) as a colourless low mp solid, mp 27–30°C. $[\alpha]_D^{20} = -76$ (0.3 g/100 mL, EtOH). Found: C, 66.5; H, 6.9; N, 8.3, C₂₉H₃₅N₃O₆ requires: C, 66.75; H, 6.8; N, 8.05; δ (300 MHz): 7.84–7.20 (m, 7H, ArH), 5.51 (m, 1H, H₁'), 4.80 (d, 1H, *J*=7.7 Hz, H_A), 4.52 (m, 1H, H₄''), 3.85–3.45 (m, 4H), 3.22 (m, 1H, H₄'), 3.16 (s, 3H, CO₂Me), 2.9 (m, 1H), 2.6–1.5 (m, 7H) and 1.49 (s, 9H, O^tBu); *m/z* (%) (FAB): 522 (M+1, 27), 466 (8), 153 (100) and 69 (47).

4.3.2. Cycloadduct 10b (2R,4S,5R,1'S). After a reaction time of 4 h and work up the product (86%) crystallised from petroleum ether (60–80) as a low mp solid, mp 37–40°C; $[\alpha]_D^{20} = -92.8$ (0.5 g/100 mL, EtOH). Found: C, 59.45; H, 7.30; N, 8.9; C₂₅H₃₃N₃O₆·2H₂O requires: C, 59.25; H, 7.30; N, 8.7%. HRMS (EI), found: 471.2380; C₂₅H₃₃N₃O₆ requires: 471.2370; δ (300 MHz): 7.15 (m, 5H, ArH), 5.50 (m, 1H, H₁'), 4.80 (d, 1H, *J*=8.0 Hz, H_A), 4.50 (m, 1H, H₄''), 3.75 (m, 3H), 3.45 (m, 3H, H₄'), 3.34 (s, 3H, CO₂Me), 2.9 (m, 1H), 2.82 (m, 1H), 2.5–1.6 (m, 5H) and 1.48 (s, 9H, O^tBu); *m/z* (%) (FAB): 471 (M⁺, 62), 416 (22), 342 (29), 258 (44), 239 (100), and 55 (86).

4.3.3. Cycloadduct 12a (1S,2R,4S,5R,1'S). After a reaction time of 4 h and work up the product (81%) crystallised from petroleum ether (60–80) ether as colourless needles, mp 103–105°C. $[\alpha]_D^{20} = -192$ (0.5 g/100 mL, EtOH). Found: C, 68.4; H, 7.9; N, 6.35, C₃₉H₅₀N₃O₇·0.5H₂O requires: C, 68.6; H, 7.5; N, 6.15%; δ (300 MHz): 7.93–7.41 (m, 7H, Ar-H), 5.6 (d, 1H, *J*=3.9 Hz, H_D), 5.28 (m, 1H, H₁'), 4.70 (dd, 1H, *J*=4.4, 9.7 Hz, H_A), 4.52 (m, 1H, H₄''), 3.87 (m, 1H, H₇''), 3.55 (m, 2H, H_B+menthyl-CHO), 3.40 (m, 1H, H₄'), 3.02 (dd, 1H, *J*=4.0, 8.0 Hz, H_C), 3.6 (m, 1H, H₇''), 2.43–1.6 (m, 15H), 1.49 (s, 9H, O^tBu), 0.62 (d, 3H, *J*=6.6 Hz, CHMe), 0.83 and 0.95 (2×d, 6H, *J*=6.9 Hz, CHMe₂); *m/z* (%)

(FAB): 674 (M+1, 40), 462 (19), 240 (38), 206 (50), 153 (100), 83 (52) and 55 (72).

4.3.4. Cycloadduct 12b (1S,2R,4S,5R,1'S). Reaction time 5 h. After work up the product (89%) crystallised from ether–hexane–ethanol as colourless prisms, mp 83–87°C. $[\alpha]_D^{20} = -188.8$ (0.5 g/100 mL, EtOH). Found: C, 65.3; H, 8.0; N, 8.9, $C_{34}H_{47}N_4O_7$ requires: C, 65.35; H, 7.75; N, 8.95%; δ (300 MHz): 8.6 (d, 1H, pyridine-H), 7.7 (m, 1H, pyridine-H) 7.4 (d, 1H, pyridine-H), 7.13 (m, 1H, pyridine-H), 5.58 (d, 1H, $J=4.1$ Hz, H_D), 5.3 (m, 1H, H'), 4.66 (m, 2H, H_A and H_4''), 3.90 (d, 1H, $J=9.7$ Hz, H_B), 3.81 (m, 1H, H_7'), 3.61 (m, 2H, menthyl-CHO+menthyl-H), 3.45 (m, 1H, H_4'), 3.12 (dd, 1H, $J=4.2, 8.1$ Hz, H_C), 2.43–1.6 (m, 15H), 1.49 (s, 9H, O'Bu), 0.60 (d, 3H, $J=6.7$ Hz, CHMe), 0.88 and 0.95 (2xd, 6H, $J=6.9$ Hz, CHMe₂); m/z (%) (FAB): 625 (M+1, 100), 495 (16), 469 (24), 413 (17), 97 (37), 83 (74) and 55 (94).

4.3.5. Cycloadduct 12c (1S,2R,4S,5R,1'S). Reaction time 5 h. After work up the product (93%) crystallised from hexane–ethanol as colourless prisms, mp 205–207°C. $[\alpha]_D^{20} = -195.2$ (0.5 g/100 mL, EtOH). Found: C, 66.95; H, 8.0; N, 6.50 $C_{35}H_{49}N_3O_7$ requires: C, 67.35; H, 7.90; N, 6.75%. HRMS (EI), found: 623.3565, $C_{35}H_{49}N_3O_7$ requires: 623.3570; δ (300 MHz): 7.51–7.15 (m, 5H, Ar-H), 5.54 (d, 1H, $J=4.0$ Hz, H_D), 5.25 (m, 1H, H_1'), 4.64 (dd, 1H, $J=4.2, 9.4$ Hz, H_A), 4.51 (m, 1H, H_4''), 3.81 (m, 1H, H_7'), 3.51 (m, 1H, menthyl-CHO), 3.48 (m, 2H, H_B and H_4'), 3.02 (dd, 1H, $J=3.8, 7.8$ Hz, H_C), 2.53 (m, 1H, H_7''), 2.48–1.52 (m, 16H), 1.48 (s, 9H, O'Bu), 0.68 (d, 3H, $J=6.9$ Hz, CHMe), 0.83 and 0.92 (2xd, 6H, $J=6.8$ Hz, CHMe₂); m/z (%) (FAB): 624 (M+1, 45), 412 (16), 153 (30), 97 (38), 83 (69) and 55 (100).

4.4. Single-crystal X-ray analyses

Crystallographic data for both **8a** and **12c** were measured on a Nonius Kappa CCD area-detector diffractometer using a mixture of area detector ω - and ϕ -scans and graphite monochromated Mo K_α radiation ($\lambda=0.71073$ Å). Both structures were solved by direct methods using SHELXS-86¹⁹ and were refined by full-matrix least-squares (based on F^2) using SHELXL-97.^{20,21} The weighting scheme used was $w=[\sigma^2(F_o^2)+(xP)^2+yP]^{-1}$ where $P=(F_o^2+2F_c^2)/3$. All non-hydrogen atoms of both structures were refined with anisotropic displacement parameters whilst hydrogen atoms were constrained to predicted positions using a riding model. The residuals wR_2 and R_1 , given below, are defined as $wR_2=(\sum[w(F_o^2-F_c^2)^2]/\sum[wF_o^2])^{1/2}$ and $R_1=\sum||F_o|-|F_c||/\sum|F_o|$.

Crystal data for 8a. $C_{30}H_{34}N_4O_6$, 0.70×0.23×0.13 mm, $M=546.61$, orthorhombic, space group $P2_12_12_1$, $a=12.4953(1)$, $b=15.9514(2)$, $c=16.1880(2)$ Å, $U=3226.55(6)$ Å³, $Z=4$, $D_c=1.13$ Mg m⁻³, $\mu=0.08$ mm⁻¹, $F(000)=1160$, $T=150$ K.

Data collection. $1.0 < 2\theta < 52.0^\circ$; 6302 unique data were collected [$R_{int}=0.058$]; 6081 reflections with $F_o > 4.0\sigma(F_o)$.

Structure refinement. Number of parameters=370, goodness of fit, $s=1.071$; $wR_2=0.1014$, $R_1=0.0368$.

Crystal data for 12c. $C_{35}H_{49}N_3O_7 \cdot CH_2Cl_2$, 0.48×0.11×0.10 mm, $M=708.7$, orthorhombic, space group $P2_12_12_1$, $a=9.6778(1)$, $b=15.4738(2)$, $c=24.5585(3)$ Å, $U=3677.69(8)$ Å³, $Z=4$, $D_c=1.28$ Mg m⁻³, $\mu=0.23$ mm⁻¹, $F(000)=1512$, $T=150$ K.

Data collection. $1.0 < 2\theta < 52.0^\circ$; 7045 unique data were collected [$R_{int}=0.058$]; 6602 reflections with $F_o > 4.0\sigma(F_o)$.

Structure refinement. Number of parameters=440, goodness of fit, $s=1.047$; $wR_2=0.1129$, $R_1=0.0467$.

Full supplementary crystallographic data, which include hydrogen co-ordinates, thermal parameters and complete bond lengths and angles, have been deposited at the Cambridge Crystallographic Data Centre (**8a**, CCDC 167657; **12c**, CCDC 167658) and are available on request.

Acknowledgements

We thank Leeds University, Mersin University for support and Technical Research Council of Turkey–The Royal Society–UK (TUBITAK-ESEP-Royal Society) for a scholarship to Dr H. Ali DONDAS and Roche for a generous gift of starting material **5**.

References

- Gante, J. *Angew. Chem., Int. Ed. Engl.* **1994**, *33*, 1699–1720.
- Olson, G. L.; Bolin, D. R.; Bonner, M. P.; Bos, M.; Cook, C. M.; Fry, D. C.; Graves, B. J.; Hatada, M.; Hill, D. E.; Kahn, M.; Madison, V. S.; Rusiecki, V. K.; Sarabu, R.; Sepinwall, J.; Vincent, G. P.; Voss, M. E. *J. Med. Chem.* **1993**, *36*, 3039–3049.
- Olson, G. L.; Voss, M.; Hill, D. E.; Kahn, M.; Madison, V. S.; Cook, C. M. *J. Am. Chem. Soc.* **1990**, *112*, 323–333.
- Gavra, S. H.; Brunner, H. R.; Turini, G. A. *N. Engl. J. Med.* **1978**, *298*, 991–995.
- Natoff, I. L.; Attwood, M. R.; Eichler, D. A.; Kogler, P.; Kleinbloesem, C. H.; Brummelen, P. V. *Cardiovasc. Drug Rev.* **1985**, *569*, 580.
- Natesh, R.; Schwager, S. L.; Sturrock, E. D.; Acharya, K. R. *Nature* **2003**, *421*, 551–554.
- Tipnis, S. R.; Hooper, N. M.; Hyde, R.; Karran, E.; Christie, G.; Turner, A. J. *J. Biol. Chem.* **2000**, *275*, 33238–33243.
- Crackower, M. A.; Seroo, R.; Oudit, E. Y.; Yagil, C.; Kozieradzki, I.; Scanga, S. E.; Oliveira-dos-Santos, A. J.; da Costa, J.; Zhang, L.; Pei, Y.; Scholey, J.; Ferrario, C. M.; Manoukian, A. S.; Chappell, M. C.; Baxx, P. H.; Yogil, Y.; Penninger, J. M. *Nature* **2002**, *417*, 822–828.
- Guy, J. L.; Jackson, R. M.; Acharya, K. R.; Sturrock, E. D.; Hooper, N. M.; Turner, A. J. Submitted for publication.
- Attwood, R. M.; Hassall, C. H.; Kröhn, A.; Lawton, G.; Redshaw, S. *J. Chem. Soc., Perkin Trans. 1* **1986**, 1011–1019.
- Thomas, W. A.; Gilbert, P. J. *J. Chem. Soc., Perkin Trans. 2* **1985**, 1077–1082.
- Thomas, W. A.; Whitcombe, I. W. A. *J. Chem. Soc., Perkin Trans. 2* **1986**, 747–755.
- Grigg, R.; Sridharan, V. *Advances in Cycloaddition*, JAI Press Inc: New York, 1993; Vol. 3, pp 161–204.
- Barr, D. A.; Dorrity, M. J.; Grigg, R.; Hargreaves, S.; Malone,

- J. F.; Montgomery, J.; Redpath, J.; Stevenson, P.; Thornton-Pett, M. *Tetrahedron* **1995**, *51*, 273–294.
13. Dondas, H. A.; Grigg, R.; Thornton-Pett, M. *Tetrahedron* **1996**, *52*, 13455–13466.
14. Grigg, R.; McMeekin, P.; Sridharan, V. *Tetrahedron* **1995**, *51*, 13347–13356.
15. We thank Roche-UK for a generous gift of **5**.
16. Barr, D. A.; Dorrity, M. J.; Grigg, R.; Hargreaves, S.; Malone, J. F.; Montgomery, J.; Redpath, J.; Stevenson, P.; Thornton-Pett, M. *Tetrahedron* **1995**, *51*, 273–294.
17. Grigg, R.; McMeekin, P.; Sridharan, V. *Tetrahedron* **1995**, *51*, 13347–13356.
18. Cooper, D. M.; Grigg, R.; Hargreaves, S.; Kennewell, P.; Redpath, J. *Tetrahedron* **1995**, *51*, 7791–7808.
19. Sheldrick, G. M. *Acta Crystallogr.* **1990**, *A46*, 467–473.
20. Sheldrick, G. M. *SHELX-93. Program for Refinement of Crystal Structures*; University of Göttingen: Germany, 1993.
21. Flack, H. *Acta Crystallogr., Sect. A* **1983**, *39*, 876–881.